Correspondence

Generalized Multichannel Image-Filtering Structures

Damianos G. Karakos and Panos E. Trahanias

***Abstract*— Recent works in multispectral image processing advocate the employment of vector approaches for this class of signals. Vector processing operators that involve the minimization of a suitable error criterion have been proposed and shown appropriate for this task. In this framework, two main classes of vector processing filters have been reported in the literature. In [1], Astola *et al.* introduce the well-known class of *vector median filters* (VMF), which are derived as maximum likelihood (ML) estimates from exponential distributions. In [2] and [3], the authors study the processing of color image data using directional information, considering the class of vector directional filters (VDF). In this paper, we introduce a new filter structure, the *directional-distance filters* (DDF), which combine both VDF and VMF in a novel way. We show that DDF are robust signal estimators under various noise distributions, they have the property of chromaticity preservation and, finally, compare favorably to other multichannel image processing filters.**

I. Introduction

In multichannel, and especially color image processing, it is accepted that the vector approach is more appropriate compared to traditional approaches that have addressed componentwise operators. This is due to the inherent correlation that exists between the image channels [4], [5]. In vector approaches, each pixel value is considered as an m-dimensional vector (m is the number of image channels; in the case of color images, $m = 3$), whose characteristics, i.e., magnitude and direction, are examined. The vectors' direction signifies their chromaticity, while their magnitude is a measure of their brightness. This approach has attracted much research lately since it is very well suited for the elimination of noise [4], [6]–[8], and other tasks, such as restoration [9], [10], edge enhancement [11], edge detection [12], [13] and segmentation [14]. A number of vector processing filters usually involve the minimization of an appropriate error criterion [1]–[3], [15], [16]. Such filters can be broadly characterized by the vector attribute they consider. One class of filters considers the distance in the vector space between the image vectors; typical representative of this class is the *vector median filter* (VMF) [1]. A second class of filters operate by considering the vectors' direction, and hence the name *vector directional filters* (VDF's) [2], [3].

VMF's are derived as MLE estimates from exponential distributions [1], while VDF's are spherical estimators (sample spherical median) when the underlying distribution is a spherical (directional) one [3]. The former—VMF's—perform accurately when the noise follows a *long-tailed* distribution (e.g. exponential or impulsive); moreover, any outliers in the image data are easily detected and eliminated by VMF's. The latter—VDF's—are optimal directional estimators and consequently are very effective in preserving the chromaticity of the image vectors [3]. A drawback of VDF lies in the fact that they do not consider the magnitude of the image vectors; to alleviate for that they operate in cascade with a grey-scale filter, which accounts for the vectors' magnitude. Depending on the choice of the grey-scale filter, VDF's can be very effective for various noise distributions [3]. However, the resulting filter structures are complex and the corresponding implementations may be slow since they operate in two steps.

(a)

(b)

Fig. 1. Test color images. (a) Bird image. (b) Peppers image.

In this paper, a novel filter structure is introduced, the *directional-distance filters* (DDF's). DDF's constitute a generalization of VMF's and VDF's, and are derived by a joint minimization of the functions that define VMF's and VDF's [17]. Directional-distance filters are very useful in color (and generally multichannel) image processing, since they inherit the properties of their ancestors. They constitute very accurate estimators in *long-* and *short-tailed* noise distributions and, at the same time, they preserve the chromaticity of the image vectors. Moreover, they eliminate the second step (grey-scale filter) required in VDF's, resulting in simple and fast filter structures. DDF's bear similarities to multichannel filters that employ varied error

Manuscript received April 5, 1996; revised February 19, 1997. The associate editor coordinating the review of this manuscript and approving it for publication was Prof. H. Joel Trussell.

D. G. Karakos is with the Institute for Systems Research and Department of Electrical Engineering, University of Maryland, College Park, MD 20742 USA (e-mail: karakos@isr.umd.edu).

P. E. Trahanias is with the Institute of Computer Science, Foundation for Research and Technology–Hellas, 711 10 Heraklion, Crete, Greece and the Department of Computer Science, University of Crete, 714 09 Heraklion, Crete, Greece (e-mail: trahania@ics.forth.gr).

Publisher Item Identifier S 1057-7149(97)04863-X.

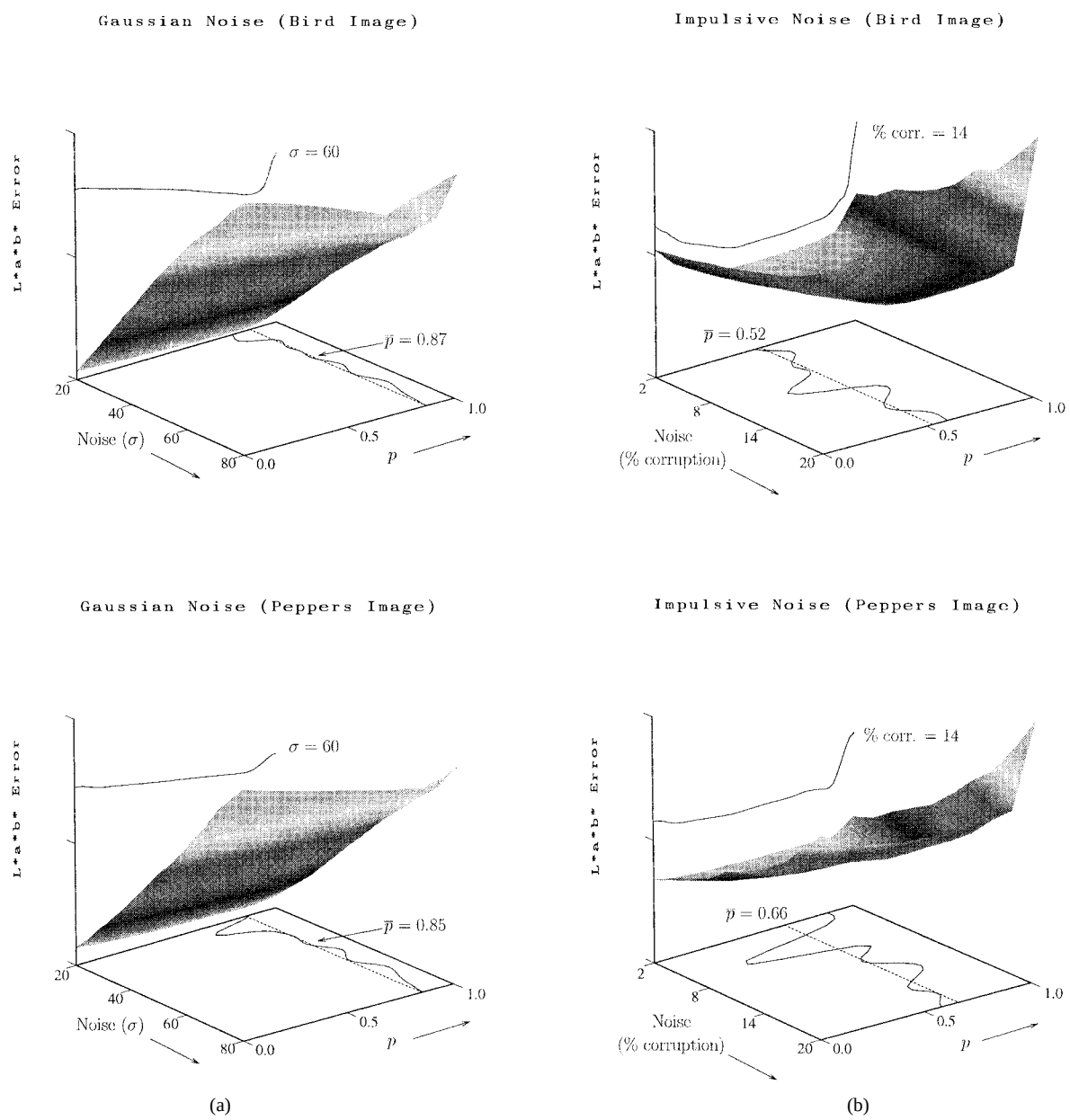

Fig. 2. Error surfaces for $p \in [0, 1]$. (a) Gaussian noise. (b) Impulsive noise.

criteria in the filtering process [7], [15]. However, such structures use local measures to select the optimal processing at each image site, whereas, DDF's operate independently of such measures by appropriately combining two criteria.

In the following sections, DDF's are first introduced as a generalization of VMF's and VDF's. Since DDF's assume the product of two factors, a study is then performed to derive the significance of each of these factors. This is based on experimental simulations under various noise models and reveals the importance of directional information in color image processing. Moreover, it provides the operating bounds of DDF. Comparative and illustrative results follow that demonstrate the accurate performance and generality of DDF. Concluding remarks are finally presented that summarize the results of this work.

II. Review of Relevant Work and Definitions

Let W be the processing window of size n and let $x_i,\ i = 1, 2, \cdots, n$ be the pixels in W. Let also the (vector-valued) image function at pixel x_i be denoted as $\mathbf{f}_i$. The following two definitions introduce VMF's and VDF's, respectively (both definitions are valid in the case of m-dimensional image functions, $m \geq 2$)

Definition 1: [1] Let the input set $\{\mathbf{f}_i, i = 1, 2, \cdots, n\}$ and let L_i correspond to $\mathbf{f}_i$ and be defined as

$$L_i = \sum_{j=1}^{n} ||\mathbf{f}_i - \mathbf{f}_j||, \quad i = 1, 2, \cdots, n \tag{1}$$

where $||.||$ is an appropriate vector norm. The vector $\mathbf{f}_i$ for which $L_i \leq L_j,\ \forall\ j = 1, 2, \cdots, n$, is the output of the VMF. In other words, the VMF outputs the vector that minimizes the sum of the distances to all the other vectors.

An analogous definition holds for the *basic vector directional filter* (BVDF) [2], by incorporating the *vector angles* instead of the *vector distances*.

Definition 2: [2], [3] Let the input set $\{\mathbf{f}_i, i = 1, 2, \cdots, n\}$ and let α_i correspond to $\mathbf{f}_i$

$$\alpha_i = \sum_{j=1}^{n} \mathcal{A}(\mathbf{f}_i, \mathbf{f}_j), \quad i = 1, 2, \cdots, n \tag{2}$$

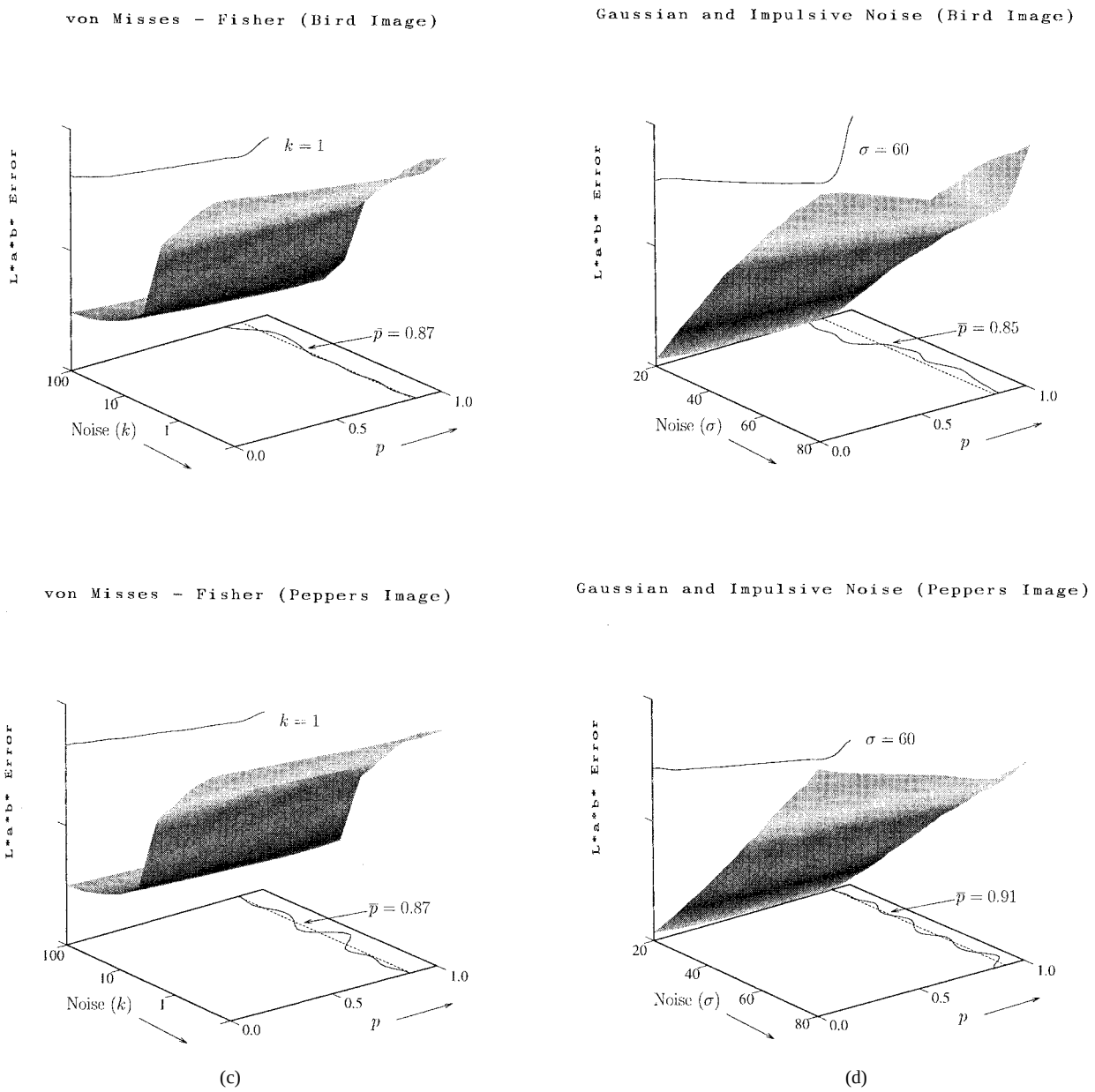

(c) (d)

Fig. 2 (*Continued*). Error surfaces for $p \in [0, 1]$. (c) Von Misses–Fisher noise. (d) Mixture of Gaussian and impulsive noise.

where $\mathcal{A}(\mathbf{f}_i, \mathbf{f}_j)$ denotes the angle between $\mathbf{f}_i$ and $\mathbf{f}_j$. An ordering of the α_is

$$\alpha_{(1)} \leq \alpha_{(2)} \leq \cdots \leq \alpha_{(k)} \leq \cdots \leq \alpha_{(n)} \tag{3}$$

implies the same ordering to the corresponding $\mathbf{f}_i$s

$$\mathbf{f}^{(1)} \leq \mathbf{f}^{(2)} \leq \cdots \leq \mathbf{f}^{(k)} \leq \cdots \leq \mathbf{f}^{(n)}. \tag{4}$$

The output of the BVDF is $\mathbf{f}^{(1)}$, i.e., the vector that minimizes the sum of the angles with all the other vectors (sample spherical median). The set of the first k vectors in the above ordered sequence [see (4)] is the output of the generalized vector directional filter (GVDF).

It is obvious from the above definition that the output of GVDF should subsequently be passed through a second filter in order to produce a single output vector. This issue has been studied in detail elsewhere [2], [3]; it has been shown that the second filter can be a *gray-scale* filter which considers only the magnitudes of the set of vectors $\mathbf{f}^{(i)}, i = 1, \cdots, k$ in the GVDF output set. Equations (1) and (2) may give rise to ambiguities, since two or more vectors may result as candidate filter outputs. Such ties are resolved arbitrarily, with an exception the case when the vector at the central window pixel (pixel under consideration) is a candidate filter output; in this case, this vector is given priority over all other candidates.

Definitions (1) and (2) indicate that the two filters (VMF, VDF) differ only in the quantity that is minimized. Both minimizations are useful, since they result in filtering structures that offer desirable features in image processing [1]–[3]. To incorporate the properties of both, we propose to combine the distance sum criterion and the angle sum criterion in the minimization formula. A straightforward way of doing that is to minimize their product $L \cdot \alpha$ (other monotonous two-variable functions could also be used in the place of "$\cdot$"). Although minimization of the product $L \cdot \alpha$ does not necessarily imply a minimum for either of the two factors (L or α), it results, however, in very small values for both of them. Therefore, the product minimization will select as the output vector the one that results in very small distance sum (L) and, at the same time, very small angle sum (α). Ties in this case are resolved in exactly the same way as above.

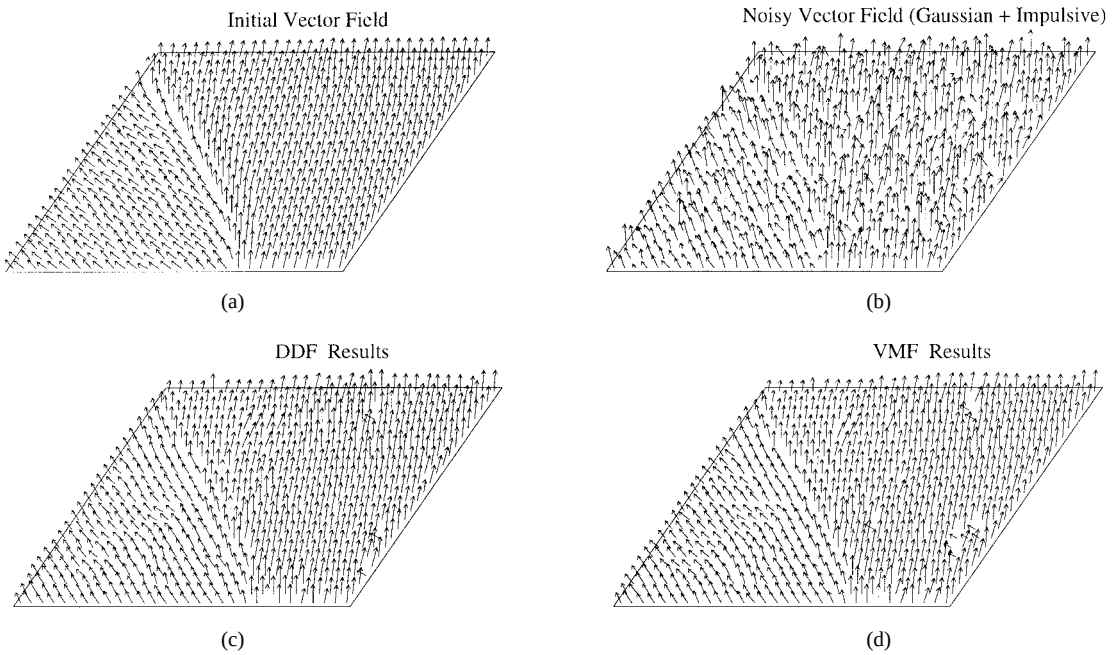

Fig. 3. Vector field for the window shown in Fig. 1(b). (a) Initial. (b) Mixture of Gaussian and impulsive noise. (c) DDF results. (d) VMF results.

Definition 3: Let the input set $\{\mathbf{f}_i, \quad i = 1, 2, \cdots, n\}$ and let Ω_i correspond to $\mathbf{f}_i$

$$\Omega_i = L_i \cdot \alpha_i = \left[\sum_{j=1}^{n} ||\mathbf{f}_i - \mathbf{f}_j||\right] \cdot \left[\sum_{j=1}^{n} \mathcal{A}(\mathbf{f}_i, \mathbf{f}_j)\right], \quad i = 1, 2, \cdots, n. \quad (5)$$

The input vector $\mathbf{f}_i$ that minimizes Ω_i is the output of the directional-distance filter (DDF).

Equation (5) can be further generalized by introducing different powers in the two factors L, α (in its current form it implies the power **one** for each of the two factors). Since we would like to derive a general scheme that has (1) and (2) as special cases, we rewrite (5) as

$$\Omega_i = L_i^{1-p} \cdot \alpha_i^p = \left[\sum_{j=1}^{n} ||\mathbf{f}_i - \mathbf{f}_j||\right]^{1-p} \cdot \left[\sum_{j=1}^{n} \mathcal{A}(\mathbf{f}_i, \mathbf{f}_j)\right]^p \quad p \in \{0, 1\}, \quad i = 1, 2, \cdots, n. \quad (6)$$

The above definition (6) is indeed quite general, having VMF and BVDF as special cases. However, its main usefulness stems from the fact that it combines both error criteria (distance sum, angle sum) in the minimization process. As it is shown later, this results in accurate and robust performance under different noise models.

III. Operation Tuning

Referring to (6), we observe that DDF depend on the parameter p, which controls the importance of the angle criterion versus the distance criterion in the overall filter structure. In the two extremes, $p = 0$ or $p = 1$, DDF behave as either VMF or BVDF, respectively. The case of $p = 0.5$ is identical with (5), giving *equal importance* to both criteria; for any other value of p, the filter is biased toward one of the two criteria.

An optimal estimation of p seems very difficult due to the two factors that are involved in the product. Moreover, for the special case of color images, we are interested in deriving accurate estimates when the error is measured in the $L^*a^*b^*$ space. $L^*a^*b^*$ is known as a space where equal color differences result in equal distances and, therefore, it is very close to human perception of colors [18]. $L^*a^*b^*$ has also been used in many studies regarding color imaging [19], [20], [3]. The transformation to the $L^*a^*b^*$ space is highly nonlinear and makes the optimal estimation of p even more difficult. Consequently, we have chosen to proceed with a computational approach for its estimation. Our approach involves the following steps.

- Four different noise models have been employed representing short- and long-tailed distributions as well as a spherical distribution. The noise models are Gaussian, impulsive, Von Misses–Fisher[1] [21], [3] and mixture of Gaussian and impulsive. These noise models were used to contaminate the test images.
- For each noise model, images were contaminated at various noise levels; the noise level has been gradually increased and, at each level, a DDF has been applied for a range of p values in the interval [0, 1] (the step in p was 0.05). The performance of DDF in each case has been measured as the mean absolute error in the $L^*a^*b^*$ space, $E_{L^*a^*b^*}$.
- The above procedure has been repeated for several color images in order to minimize any bias introduced by the individual characteristics of the images. Here, we confine our presentation to two cases: the bird and peppers color images, shown in Fig. 1.

The results obtained from the above set of experiments are graphically presented in Fig. 2 in the form of *error surfaces*. As already mentioned, the error (vertical axis) is measured in the $L^*a^*b^*$ space in order to match closely the human perception of color. The two horizontal axes represent the noise level and the parameter p, respectively. The noise axis is quantified in each case using the parameter of the corresponding noise model. In addition to the error surfaces, a cross section (one-dimensional plot projected on the $E_{L^*a^*b^*}$–p plane) is also shown in each case as a function of p for fixed noise level, to facilitate the visual observation of the error

[1] The Von Misses–Fisher distribution is the most commonly used distribution in directional data analysis [21]. It is defined parametrically, according to a concentration parameter k. For $k = 0$ it reduces to the uniform distribution on the sphere. Large values of k indicate high degree of concentration of the data.

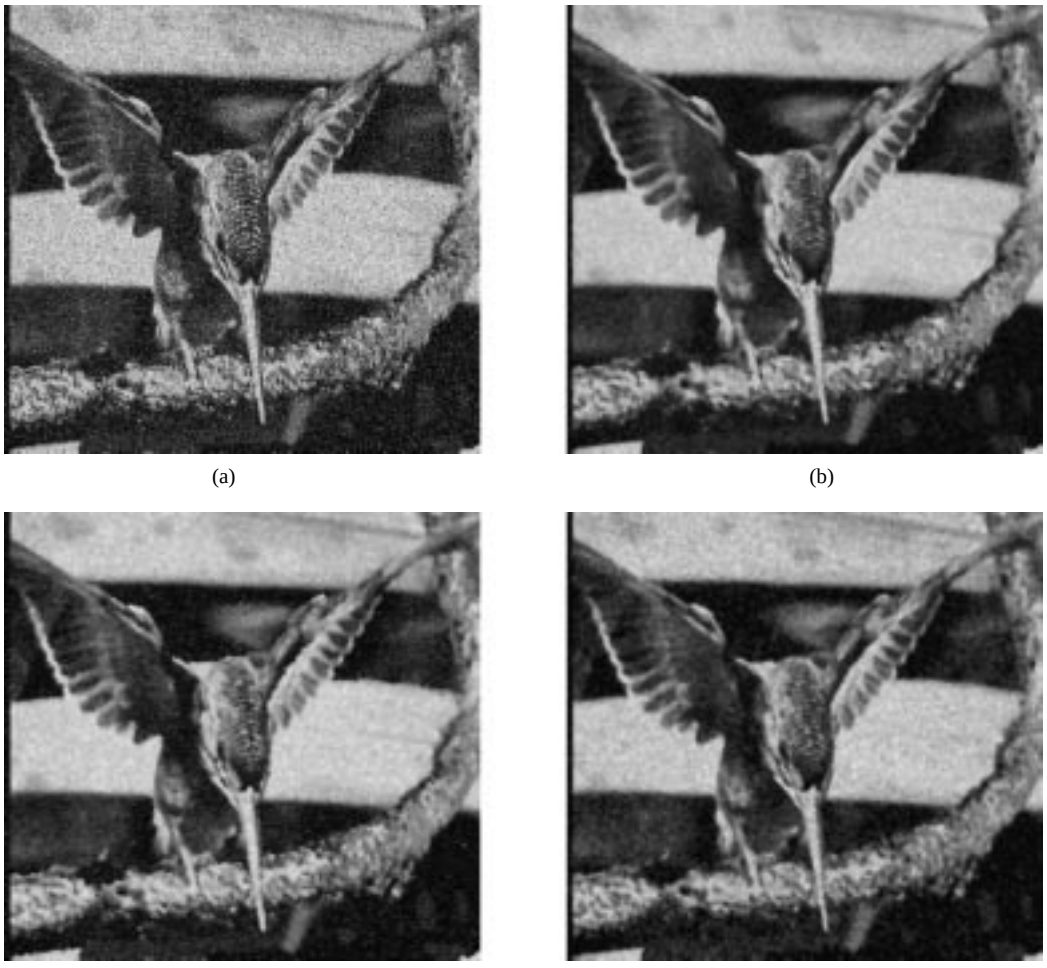

(a) (b) (c) (d)

Fig. 4. Results on the bird image [Fig. 1(a)]. (a) Mixture of Gaussian and impulsive noise. (b) DDF results. (c) VMF results. (d) VDF results.

TABLE I
$E_{L^*a^*b^*}$, GAUSSIAN NOISE (BIRD IMAGE)

	σ - Standard Deviation				
Filter	10	20	30	40	50
DDF	12.78*	13.63*	17.64	22.13	26.09
VMF	14.89	20.29	25.48	30.45	35.48
VDF	13.31	14.01	14.53*	15.56*	16.53*
R_E	15.13	21.41	28.58	36.53	45.10

TABLE II
$E_{L^*a^*b^*}$, GAUSSIAN NOISE (PEPPERS IMAGE)

	σ - Standard Deviation				
Filter	10	20	30	40	50
DDF	14.27*	16.56*	19.22*	21.74	24.55
VMF	15.08	17.52	20.71	24.21	28.07
VDF	14.91	16.82	19.25	21.54*	23.62*
R_E	15.65	19.60	25.53	34.99	45.22

surface patterns. The noise parameter for which the cross sections have been plotted is indicated on their right-end.

The surface plots of Fig. 2 present the behavior of DDF's in a compact way. The value of p that gives the minimum error value for each noise level represents the "operational" setting for the particular noise model (and color image). As can be observed, a "valley" pattern is exhibited in most of these plots that follows the direction of the noise level. This pattern illustrates the behavior of DDF's for different values of the parameter p; better performance is attained for p values corresponding to the "bottom" of the valley. The observed performance is in accordance with our intuition, since it is expected that both criteria (distance and angle) should contribute to the filtering process. This is exactly the behavior demonstrated by the error surfaces; increased filter performance is attained for values of p that consider both criteria. Moreover, since the valley pattern follows the direction of the noise level, it is verified that both criteria are important at all noise levels. Therefore, the effect of the joint minimization introduced is unambiguously demonstrated in these plots.

In order to simplify the visual detection of this valley, the points where it attains the minimum value at the corresponding noise level are drawn on the horizontal plane as a continuous curve. This curve gives the (experimentally obtained) value of p that results in optimal performance for the corresponding noise level and model. In order to obtain operational values that are constant at any noise level, the average of these values is computed and used as such; this is shown on the same plots with the dashed lines. As can be verified from these plots, the deviation of the continuous lines (true p values) from the corresponding dashed lines (averaged values) is small and, therefore, the averaged values can be safely used. Moreover, the differences in $E_{L^*a^*b^*}$ when the true or the averaged values are used are insignificant (in the order of 1% of $E_{L^*a^*b^*}$), compared to the variation of $E_{L^*a^*b^*}$ over the whole range of p values which,

TABLE III
$E_{L^*a^*b^*}$, IMPULSIVE NOISE (BIRD IMAGE)

	% of corruption				
Filter	2	6	10	14	18
DDF	11.35*	11.53*	11.69*	11.88*	12.18*
VMF	11.57	11.77	12.01	12.36	12.76
VDF	11.96	14.51	17.72	20.40	22.87
R_E	21.49	33.22	41.16	47.26	52.21

TABLE IV
$E_{L^*a^*b^*}$, IMPULSIVE NOISE (PEPPERS IMAGE)

	% of corruption				
Filter	2	6	10	14	18
DDF	13.04*	13.25*	13.46*	13.79*	14.16*
VMF	13.24	13.50	13.72	14.05	14.53
VDF	13.56	15.76	18.71	21.51	24.21
R_E	25.40	39.81	49.63	57.14	63.33

TABLE V
$E_{L^*a^*b^*}$, VON MISSES–FISHER NOISE (BIRD IMAGE)

	k				
Filter	1	5	10	20	50
DDF	21.01	17.68	17.05	16.47*	16.44*
VMF	22.27	18.70	17.98	17.57	17.27
VDF	19.69*	16.92*	16.58*	16.68	16.44
R_E	34.87	29.27	28.44	28.18	28.05

TABLE VI
$E_{L^*a^*b^*}$, VON MISSES–FISHER NOISE (PEPPERS IMAGE)

	k				
Filter	1	5	10	20	50
DDF	28.90	22.22*	21.79*	21.16*	20.75*
VMF	34.12	25.17	23.73	22.90	22.29
VDF	22.54*	22.96	21.80	21.64	21.66
R_E	45.08	35.58	33.78	32.80	32.21

TABLE VII
$E_{L^*a^*b^*}$, GAUSSIAN AND IMPULSIVE NOISE (BIRD IMAGE)

	σ - Standard Deviation				
Filter	10	20	30	40	50
DDF	16.08*	19.02*	24.79	29.63	32.89
VMF	16.89	22.12	27.86	32.87	37.82
VDF	18.15	19.09	20.45*	21.94*	23.04*
R_E	41.42	43.09	46.28	50.78	55.82

TABLE VIII
$E_{L^*a^*b^*}$, GAUSSIAN AND IMPULSIVE NOISE (PEPPERS IMAGE)

	σ - Standard Deviation				
Filter	10	20	30	40	50
DDF	16.04	18.47*	21.43*	24.14*	27.24
VMF	15.89*	18.98	22.71	26.81	28.75
VDF	20.03	21.23	23.07	24.74	26.48*
R_E	50.31	51.25	53.12	57.02	62.37

TABLE IX
NCRE, GAUSSIAN NOISE

		σ - Standard Deviation				
Image	Filter	10	20	30	40	50
Bird	DDF	8.68	9.93	11.18	12.20	13.04
	VDF	8.59*	9.81*	11.03*	12.03*	12.97*
Peppers	DDF	3.76*	4.84*	6.17*	7.51*	8.89*
	VDF	5.99	6.91	8.24	9.52	10.87

TABLE X
NCRE, IMPULSIVE NOISE

		% of corruption				
Image	Filter	2	6	10	14	18
Bird	DDF	7.44*	7.54*	7.64*	7.75*	7.91*
	VDF	7.76	8.90	10.40	11.71	12.89
Peppers	DDF	2.99*	3.09*	3.20*	3.36	3.53*
	VDF	3.02	3.10	3.21	3.35*	3.56

TABLE XI
NCRE, VON MISSES–FISHER NOISE

		k				
Image	Filter	1	5	10	20	50
Bird	DDF	14.53	12.19	11.71	11.44*	11.25*
	VDF	14.06*	11.99*	11.66*	11.53	11.46
Peppers	DDF	12.86	9.30	8.66	8.29	8.03*
	VDF	10.78*	8.63*	8.32*	8.20*	8.16

TABLE XII
NCRE, GAUSSIAN AND IMPULSIVE NOISE

		σ - Standard Deviation				
Image	Filter	10	20	30	40	50
Bird	DDF	9.44*	11.43*	13.28	14.96	16.35
	VDF	10.94	11.76	12.61*	13.38*	13.98*
Peppers	DDF	4.28*	5.69*	7.16*	8.69*	10.30*
	VDF	5.99	6.91	8.24	9.52	10.87

for moderate noise levels, was found above 15% in most cases. Actually, experimentation with different color images has revealed that $E_{L^*a^*b^*}$ remains practically unchanged for a small range of p values around its mean value.

Another important observation refers to the consistency of the "valley" location in different images. The pairs of plots in Fig. 2(a)–(d) present the same results for two images. As can be verified, very similar results are obtained (for each noise model) for the two images. This can be interpreted as the fact that, for a particular noise model, the operational value of the parameter p can be experimentally obtained.

A final comment regards the error behavior in the presence of different noise models. The plots of Fig. 2 demonstrate that additive Gaussian and mixture of Gaussian with impulsive noise favor higher values of p (the filter tends to behave more like a VDF); very similar behavior is also exhibited in the case of a spherical noise distribution (Von Misses-Fisher). When the noise is modeled as impulsive (long-tailed noise), the best filter performance is obtained for slightly smaller p values; in other words, a filter behavior closer to a VMF is favored. This illustrates the fact that the vector median is an accurate estimator in the presence of impulsive noise but still directional

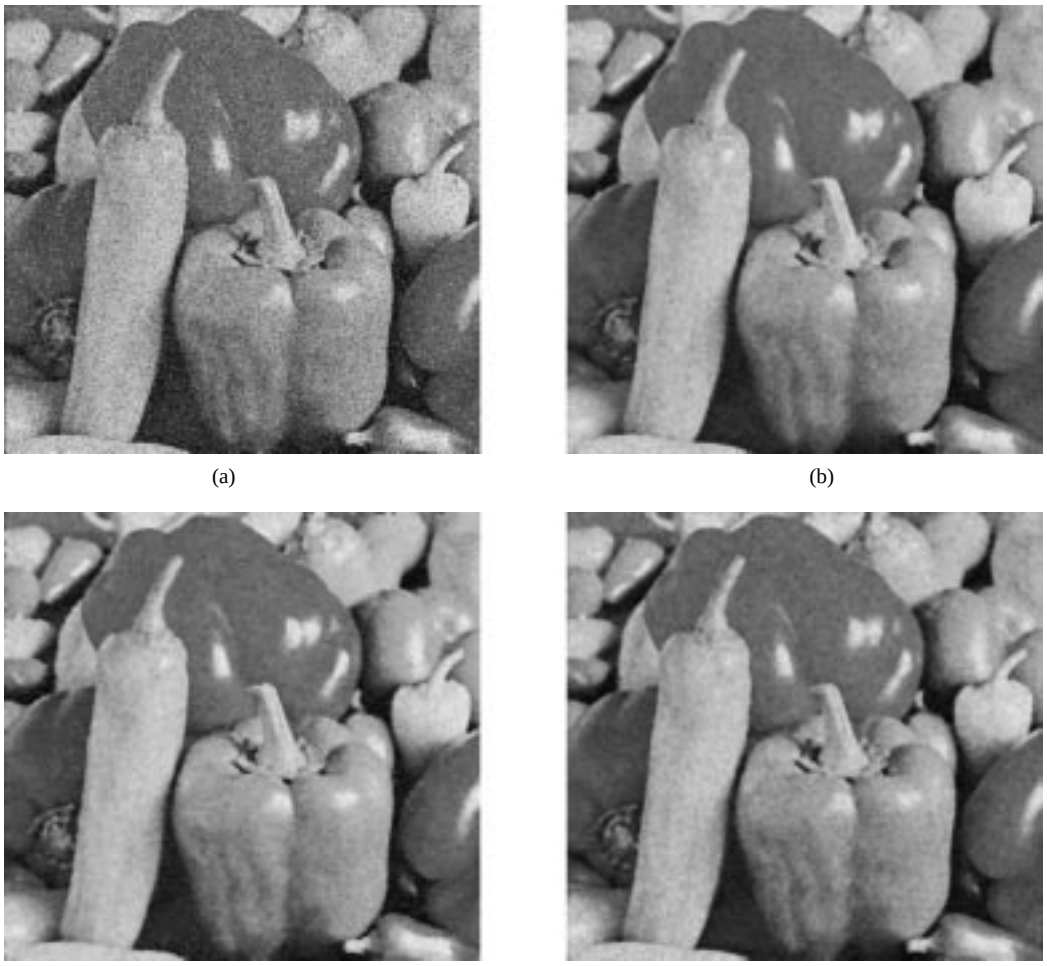

(a) (b) (c) (d)

Fig. 5. Results on the peppers image [Fig. 1(b)]. (a) Mixture of Gaussian and impulsive noise. (b) DDF results. (c) VMF results. (d) VDF results.

information is very important (when the error is measured in the $L^*a^*b^*$ space).

Based on the p values suggested by the plots of Fig. 2, we have adopted a constant operational value $p = 0.75$. This represents a compromise between the (slightly) different values implied by the different noise models. More importantly, however, since the performance measures remain practically unchanged for a range of p values, which includes the value $p = 0.75$, this is a "safe" value independent of the noise distribution.

IV. Experimental Results

The performance of DDF's has been experimentally assessed for various noise models. The error figures, measured in the $L^*a^*b^*$ space, have shown the accurate performance of DDF's and their superiority compared to VMF's and their variation, the R_E filters [16]. When compared to VDF's, they perform at least comparable and in some cases slightly better, but still they have the advantage over VDF's in that they operate in one step without involving any grey-scale filter. Many different color images were used in our simulations; here, we present sample results regarding the two images, bird and peppers, shown in Fig. 1(a) and (b).

In order to get a subjective impression of the performance of DDF's, Fig. 3 illustrates their application to a (part of a) color image, shown as a vector field. This vector field is exactly the 30×24 window shown in Fig. 1(b). The initial vector field is shown in Fig. 3(a); this has been corrupted by a mixture of Gaussian ($\sigma = 30$) and 5% impulsive noise, and the result is given in Fig. 3(b). DDF's and VMF's have been applied to the noisy image. The results are presented in Fig. 3(c) and 3(d), respectively. The accuracy of DDF's in restoring the vector field is demonstrated in this example.

Some selected results from our evaluation experiments regarding DDF's, VMF's, VDF's, and R_E filters are presented in tabular form in Tables I–VIII; in these tables the values of $E_{L^*a^*b^*}$ are given. The results refer to two color images, bird and peppers, corrupted with the four noise models mentioned in the previous section. For a fair comparison, VDF's were combined with the *best* grey-scale filter with respect to the noise model, resulting in very accurate performance [3]. An asterisk (*) in a table entry indicates the best filter performance for the corresponding noise level. As can be verified, DDF's result in better, or at least equal performance, in most cases. In some cases, VDF's perform slightly better but still they involve two steps in the filtering process (directional and magnitude processing) and their performance depends on the selection of the gray-scale filter. DDF's on the other side, are very simple filter structures and operate accurately independent of the underlying noise model.

The chromaticity preservation of DDF's has been experimentally demonstrated by measuring the *normalized chromaticity error* (NCRE), introduced in [2]. NCRE measures the error as a distance on the Maxwell triangle, i.e., the triangle drawn between the three color primaries: red, green, and blue [18]. Since the point of intersection on the Maxwell triangle serves to characterize the chromaticity of a given image vector, NCRE gives an indication of the chromaticity

error.[2] The results referring to NCRE are tabulated in Tables IX–XII for exactly the same noise models as the ones used in the $E_{L^*a^*b^*}$ measurements (Tables I–VIII). Since VDF's have been shown as very accurate chromaticity preserving filters [2], [3], only the DDF and VDF results are presented here. The other filters have generally inferior performance regarding color chromaticity. On the contrary, Tables IX–XII demonstrate that DDF's and VDF's have comparable performances in this sense. This is in accordance with our intuition, since both filters include the angles between the image vectors in their minimization criteria, thus resulting in accurate chromaticity filters.

Since the topic is *color image processing*, a subjective assessment of any filter's performance is the ultimate criterion regarding its usability. Figs. 4 and 5 present filtering results for the bird and peppers images, respectively. Fig. 4(a) shows the bird image corrupted with a mixture of Gaussian ($\sigma = 30$) and 5% impulsive noise. The filtered versions of the image with the DDF, VMF, and VDF are given in Fig. 4(b), (c), and (d), respectively. As can be observed, filtering with the DDF has resulted in a better recovery of the initial image, compared to VMF. The background, for example, in the VMF result appears more distorted and erroneous chromaticities are visible; the latter is also visible in the tree branch and the left wing (from the point of view of the observer) of the bird, where "red" colors have resulted after VMF processing. When compared to VDF, the DDF and VDF results appear almost identical; still, VDF processing exhibits a slight smoothing effect, which can be observed on the tree branch and the bird wings. This can be attributed to the grey-scale filter (α-trimmed mean) that is applied in the second step of VDF processing. The general impression, however, is that the DDF and VDF have similar filtering performances; this has already been stated throughout the paper. The advantage of DDF's over VDF's lies in that they eliminate the second step required in VDF processing and they operate independent of the underlying noise model. Analogous results are given in Fig. 5 for the color image of peppers. Again, the reader can verify that the DDF result [see Fig. 5(b)] is closer to the initial image. In the VMF result [see Fig. 5(c)], noisy colors appear more predominant, especially in the foreground peppers—two green and one red. Consequently, both results verify the superiority of the DDF in color image filtering.

V. Discussion

Multispectral image processing has been mainly treated to date as a minimization problem, by selecting suitable minimization criteria. However, these criteria have led to solutions that fit special cases. In this work, we have derived a novel filter class (DDF) by employing a combination (product minimization) of two such criteria. These criteria serve for the definition of VMF's and VDF's, respectively; therefore, DDF's have been constructed as a generalization of these two filters.

Operation tuning for the DDF has been tackled by experimentally deriving an operational value for the parameter p involved in the DDF defining equation. This has been achieved by performing exhaustive simulations in the whole range of p values, under various noise models and with different color images. In addition, these simulations have demonstrated the robustness of the DDF under different noise distributions. Our experimental results have shown the accurate performance of DDF's independent of the noise model. Moreover, they constitute chromaticity preserving operators, like their ancestors, the VDF operators. Therefore, DDF's may be a very useful and general tool in color image processing.

In this paper, DDF's have mainly been studied in the framework of color image processing. More work is needed, however, in order to address the processing of other multispectral images (i.e., satellite images and multispectral medical images). Moreover, the issue of joint minimization in the filtering process should be further investigated; the incorporation of other factors, besides the distance sum (L) and the angle sum (α), in the minimization formula (6) might result in even more effective filtering structures.

[2] NCRE should not be considered as the *exact* chromaticity error, since the Maxwell triangle is *not* a space where equal color differences result in equal distances; rather, NCRE measures the *exact* distance, which can be *qualitatively* interpreted as the chromaticity error.

References

[1] J. Astola, P. Haavisto, and Y. Neuvo, "Vector median filters,"*Proc. IEEE*, vol. 78, pp. 678–689, Apr. 1990.

[2] P. E. Trahanias and A. N. Venetsanopoulos, "Vector directional filters—A new class of multichannel image processing filters," *IEEE Trans. Image Processing*, vol. 2, pp. 528–534, Apr. 1993.

[3] P. E. Trahanias, D. Karakos, and A. N. Venetsanopoulos, "Directional processing of color images: Theory and experimental results," *IEEE Trans. Image Processing*, vol. 5, pp. 868–880, June 1996.

[4] P. E. Trahanias, I. Pitas, and A. N. Venetsanopoulos, "Color image processing," in *Control and Dynamic Systems*, C. T. Leondes, Ed. New York: Academic, 1994, vol. 67, pp. 45–90.

[5] R. Machuca and K. Phillips, "Applications of vector fields to image processing," *IEEE Trans. Pattern Anal. Machine Intell.*, vol. PAMI-5, pp. 316–329, May 1983.

[6] M. Gabbouj, E. J. Coyle, and N. C. Gallagher, "An overview of median and stack filtering," *Circuits, Syst., Signal Processing*, vol. 11, pp. 7–45, 1992.

[7] K. Tang, J. Astola, and Y. Neuvo, "Nonlinear multivariate image filtering techniques," *IEEE Trans. Image Processing*, vol. 4, pp. 788–798, June 1995.

[8] I. Pitas and P. Tsakalides, "Multivariate ordering in color image filtering," *IEEE Trans. Circuits Syst. Video Technol.*, vol. 1, pp. 247–259, Sept. 1991.

[9] N. P. Galatsanos, A. K. Katsaggelos, R. T. Chin, and A. D. Hillery, "Least squares restoration of multichannel images," *IEEE Trans. Acoust., Speech, Signal Processing*, vol. 39, pp. 2222–2236, Oct. 1991.

[10] N. P. Galatsanos and R. T. Chin, "Restoration of color images by multichannel Kalman filtering," *IEEE Trans. Acoust., Speech, Signal Processing*, vol. 39, pp. 2237–2252, Oct. 1991.

[11] K. Tang, J. Astola, and Y. Neuvo, "Multichannel edge enhancement in color image processing," *IEEE Trans. Circuits Syst. Video Technol.*, vol. 4, pp. 468–479, Oct. 1994.

[12] P. E. Trahanias and A. N. Venetsanopoulos, "Vector order statistics operators as color edge detectors," *IEEE Trans. Syst., Man, Cybern. B*, vol. 26, pp. 135–142, Feb. 1996.

[13] A. Cumani, "Edge detection in multispectral images," *CVGIP: Graphics, Models Image Processing*, vol. 53, pp. 40–51, Jan. 1991.

[14] P. E. Trahanias, D. Karakos, and A. N. Venetsanopoulos, "Directional segmentation of color images," in *Proc. 1995 IEEE Workshop Nonlinear Signal and Image Processing*, I. Pitas, Ed., Halkidiki, Greece, June 1995, pp. 515–518.

[15] S. Fotopoulos and G. Economou, "Multichannel filters using composite distance metrics," in *Proc. 1995 IEEE Workshop Nonlinear Signal and Image Processing*, I. Pitas, Ed., Halkidiki, Greece, June 1995, pp. 503–506.

[16] R. C. Hardie and G. R. Arce, "Ranking in R^p and its use in multivariate image estimation," *IEEE Trans. Circuits Syst. Video Technol.*, vol. 1, pp. 197–209, June 1991.

[17] D. Karakos and P. E. Trahanias, "Combining vector median and vector directional filters: The directional-distance filters," in *IEEE Int. Conf. Image Processing*, Washington, DC, Oct. 1995, pp. 171–174.

[18] W. K. Pratt, *Digital Image Processing*. New York: Wiley, 1991.

[19] M. J. Vrhel and H. J. Trussell, "Filter considerations in color correction," *IEEE Trans. Image Processing*, vol. 3, pp. 147–161 Mar. 1994.

[20] C. L. Grard and H. J. Trussell, "Interpolation and extrapolation for accurate color measurement," in *Proc. 1995 IEEE Int. Conf. Image Processing*, Washington, DC, Oct. 23–26, 1995, pp. 350–353.

[21] D. Ko and T. Chang, "Robust M-estimators on spheres," *J. Multivariate Anal.*, vol. 45, pp. 104–136, 1993.